

Dual black hole associated with obscured and unobscured AGN: CXO J101527.2+625911

D.-C. Kim¹, E. Momjian², Ilsang Yoon¹, Minjin Kim^{3,4}, A. S. Evans^{1,5}, Ji Hoon Kim^{6,7}, S. T. Linden⁵, L. Barcos-Munoz¹, & G. C. Privon⁸

Abstract

We report the results of an investigation to determine the nature of the offset active galactic nucleus (AGN) found in the source CXO J101527.2+625911. Hubble Space Telescope and Chandra X-ray observatory data had suggested that the offset AGN, which has an angular separation of only $0''.26$ from the center of the host galaxy, is a recoiled Super Massive Black Hole (rSMBH). We carried out high angular resolution observations with both the VLBA (1.54 GHz) and the VLA (10.0 GHz & 33.0 GHz) and detected a single compact radio source in the center of the host galaxy, with no radio continuum emission associated with the offset AGN. The detected radio source has a high brightness temperature value of $T_b = 7.2 \times 10^7$ K, indicating that the radio emission is associated with an AGN. Furthermore, we present the decomposition of high-resolution KECK spectra of the [O III]5007Å line into two narrow emission line components, which is a characteristic sign of a dual black hole system. These new radio and optical wavelength results suggest that CXO J101527.2+625911 is the host of a dual black hole system rather than a rSMBH.

¹National Radio Astronomy Observatory, 520 Edgemont Road, Charlottesville, VA 22903, USA: dkim@nrao.edu, iyon@nrao.edu, aevans@nrao.edu, stl7ey@virginia.edu, lbarcos@nrao.edu

²National Radio Astronomy Observatory, P.O. Box O, Socorro, NM 87801, USA: emomjian@nrao.edu

³Korea Astronomy and Space Science Institute, Daejeon 305-348, Korea

⁴Department of Astronomy and Atmospheric Sciences, Kyungpook National University, Daegu 702-701, Korea: mkim.astro@gmail.com

⁵Department of Astronomy, 530 McCormick Rd., University of Virginia, Charlottesville, VA 22904

⁶Metaspace, 36 Nonhyeon-ro, Gangnam-gu, Seoul 06321, Korea: jhkim@naoj.org

⁷Subaru Telescope, National Astronomical Observatory of Japan, 650 North Aohoku Place, Hilo, HI 96720, USA

⁸Department of Astronomy, University of Florida, 211 Bryant Space Sciences Center, Gainesville, FL 32611, USA: george.privon@ufl.edu

1. Introduction

A dual/binary black hole system can be formed from two interacting galaxies. The fate of the two black holes depends on a number of factors. They could merge together to form a single supermassive black hole (SMBH), or could remain a dual black hole system if the secondary galaxy loses significant fraction of its mass due to the tidal stripping effect of the primary galaxy at kpc scale (e.g. Callegari et al. 2009). Recent simulations predict that the merged SMBH can attain a recoil velocity of a few hundred to a few thousands km s^{-1} depending on mass ratios, spin magnitudes, and spin orientations of the merging SMBHs (Campanelli et al. 2007; Schnittman 2007; Baker et al. 2008; Lousto & Zlochower 2011). If the merging SMBHs are of equal mass and highly-spinning, and their spins are aligned along the orbital plane (superkick configuration), recoil velocities as large as 4000 km s^{-1} (Campanelli et al. 2007) to 5000 km s^{-1} (Lousto & Zlochower 2011) can be reached and the recoiling SMBH (hereafter rSMBH) will eventually escape from the host galaxy (i.e., Merritt et al. 2004). Studying the rSMBH is important since they will provide an essential information about how the mergers grow their bulge and black hole mass to evolve toward the normal ellipticals.

From imaging and spectroscopic surveys of the rSMBHs, ‘CXO J101527.2+625911’ was identified as a potential rSMBH candidate (Kim et al. 2017). CXO J101527.2+625911 is a QSO hosted merger remnant located at $z=0.3504$. Its morphological type is a bulge-dominated elliptical, with two nuclei in its center - a bright northern nucleus harboring AGN and is spatially offset by 1.26 kpc (0.256”) from the less bright southern nucleus that was identified as the center of the host galaxy. Spectral decomposition of the KECK spectra suggests $H\beta$ broad emission line is redshifted by $175\pm 25 \text{ km s}^{-1}$ with respect to the systemic velocity (Kim et al. 2017).

The observed spatial and velocity offsets suggest that this galaxy could be hosting a rSMBH. However, there is a possibility that this system could be a dual/binary SMBH where the second black hole is hidden behind the dust in the center of the host galaxy. To resolve whether this system has a rSMBH or a dual/binary black hole system, we have carried out Very Long Baseline Array (VLBA) and Karl G. Jansky Very Large Array (VLA) radio continuum observations.

In this paper, we report the results of our VLBA and VLA observations. The observations and data reduction are described in Section 2, the discussion is presented in Section 3, and a summary is presented in Section 4. Throughout this paper, the cosmology $H_0 = 70 \text{ km s}^{-1} \text{ Mpc}^{-1}$, $\Omega_M = 0.3$, and $\Omega_\Lambda = 0.7$ is adopted. At the distance of the target source, 1” subtends 4.94 kpc on the sky.

2. Observations and Data Reduction

The observations of the target source CXO J101527.2+625911 were conducted with the VLA and the VLBA of the National Radio Astronomy Observatory (NRAO)¹. Table 1 summarizes the observations. Details of the observations with both facilities are described separately below.

2.1. VLBA

The VLBA observations of CXO J101527.2+625911 were carried out on 2017 October 15. We utilized the ROACH Digital Backend and the polyphase filterbank (PFB) digital signal-processing algorithm to deliver eight 32 MHz data channel pairs, both with right- and left-hand circular polarizations. The data recorded at each station were sampled at 2 bits. The total observing time was 3.56 hours, and the total bandwidth was 256 MHz centered at 1.54 GHz.

The observations utilized nodding-style phase referencing with a cycle time of 3 minutes: two minutes on the target source and one minute on the phase calibrator J1019+6320. This calibrator is located at an angular distance of 0.6° from the target source CXO J101527.2+625911. The strong calibrator source 3C 147 was observed as a fringe finder and to calibrate the band-pass response. The amplitude scale of the data was calibrated using measurements of the antenna gain and the system temperatures. The data were correlated with the VLBA software correlator (Deller et al. 2011) in Socorro, New Mexico, with a 4 second correlator integration time.

In phase referenced observations, such as those presented here, the accuracy in the position of the phase calibrator determines the accuracy of the absolute position of the target source (Walker 1999). The uncertainty in the position of the phase calibrator J1019+6320 is 0.36 mas and 0.72 mas in right ascension and declination, respectively (Ma et al. 2009). Furthermore, phase referencing, as employed in our observations, is known to preserve the absolute astrometric positions to better than 10 mas (Fomalont 1999).

The editing, calibration, and imaging of the data were performed using the Astronomical Image Processing System (AIPS; Greisen 2003) following standard Very Long Baseline Interferometry data reduction procedures. The final VLBA continuum image was made with

¹The National Radio Astronomy Observatory is a facility of the National Science Foundation operated under cooperative agreement by Associated Universities, Inc.

a robust factor of 1 in the AIPS task IMAGR.

2.2. VLA

The VLA A-configuration ($B_{max} = 36.4$ km) observations of CXO J101527.2+625911 were carried out on 2018 March 7 in the X (8 – 12 GHz) and Ka (26.5 – 40 GHz) frequency bands. Utilizing the 3-bit samplers, the observations delivered a total of 8 GHz bandwidth at Ka-band centered at 33 GHz, and a total of 4 GHz bandwidth at X-band centered at 10 GHz. The flux density scale calibrator and bandpass calibrator was 3C 286, and the complex gain calibrator was J0921+6215. Both X- and Ka-band data sets were edited and calibrated using the Common Astronomy Software Applications (CASA) package version 5.1. In order to improve the calibration for the science target, we also performed two rounds of phase-only self-calibration. The final continuum images were made with Briggs weighting and a robust factor of 0.5 in the CASA task tclean.

3. Result and Discussion

Fig. 1a shows Hubble Space Telescope (HST) Advanced Camera for Surveys (ACS) I-band (F775W) image of the nuclear region in CXO J101527.2+625911, where green plus marks are the positions of the two nuclei: a northern nucleus (offset AGN) and a southern nucleus (center of the host galaxy). The white dot represents the center of the Chandra X-ray emission and the circle represents its positional uncertainty. Fig. 1b is a zoomed-in image of Fig. 1a, where white and blue contours represent the continuum emission at 33 GHz measured with the VLA, and the 1.54 GHz measured with the VLBA. Fig. 1c is a zoomed-in image of Fig. 1b, where synthesized beams are plotted on the bottom left (VLA) and bottom right (VLBA). The synthesized beam sizes are $0''.0125 \times 0''.005$ and $0''.06 \times 0''.05$ for the VLBA and VLA 33 GHz images, respectively. In both the VLBA and VLA observations, we have detected a single compact radio source near the center of the southern nucleus (host galaxy). The coordinates and flux densities of the radio source are summarized in Table. 1. Assuming the positional uncertainty of the VLA image is about 10% of the FWHM of the synthesized beam, then the VLBA and VLA radio emissions are originating from the same location. The absolute astrometry of the HST ACS images ($\sim 0''.3$) is slightly larger than the nuclear separation ($0''.265$). To identify where the location of the radio emission corresponds in the HST ACS image, we first referenced the GAIA Data Release 2 Catalogue (Gaia Collaboration 2018). The coordinates of the offset AGN (northern nucleus) identified from the GAIA Catalog are R.A.=10h15m27.2652s \pm 0.0002s and Dec.=62d59'11.6095'' \pm 0.0003''. Next, we regis-

tered this position with the northern nucleus in the HST image and measured the coordinates of the southern nucleus and found that the coordinates are R.A.=10h15m27.264s \pm 0.0002s and Dec.=62d59'11.345'' \pm 0.0003''. Thus, the positional offset between the VLBA center and the center of the host galaxy is about 0'.045 and corresponds to physical scale of 350 pc.

3.1. A rSMBH or a dual/binary SMBH?

Previously in Kim et al. (2017), we have identified this source as a possible recoiling supermassive black hole (rSMBH) mainly because the X-ray emission is associated with the offset AGN and no sign of AGN emission at optical wavelengths is detected in the nucleus of the host galaxy, though a deeply buried AGN is still possible. As discussed in the previous section, we have detected the radio emission near the center of the host galaxy. In general, radio continuum emission may originate from starbursts activities (SNe, outflows, shocks, etc...), or AGN activity. The 1.54 GHz VLBA observations reveal a continuum source with a brightness temperature $T_b = 7.2 \times 10^7$ K. Such a high brightness temperature value clearly indicates that the radio emission is AGN related (e.g., Condon et al. 1991; Condon 1992).

The detection of an optically hidden AGN in the host galaxy, as revealed through the VLBA observations, suggests that this is a dual or binary black hole system with an obscured AGN (southern nucleus) and an unobscured AGN (northern offset AGN). A commonly adopted method for selecting black hole pair candidates is to identify a pair of narrow emission lines (e.g. [O III]5007 line) in the QSO spectra. Thus, if this system is indeed a dual/binary black hole system, we could see two sets of narrow emission lines in the spectra. In the SDSS spectra (Fig. 2a), it is hard to tell if there exist two kinematically separated narrow emission lines, since a single Gaussian component (blue line) fits well to the [O III]5007 line. However, if we fit a single Gaussian to the [O III]5007 line in high-resolution KECK spectra (Fig. 2b), we see an extra component in the red part of the spectra (indicated by the arrow in the plot) - this is possible evidence that two narrow emission lines could be closely overlapped. To test this, we tried spectral decompositions using one [O III] component line versus two [O III] component lines and compared the results. In the fit, we added an [O III] blue asymmetry component that is often observed in QSOs and interpreted as evidence of an outflow. The fitting results are plotted in Figure 3a (one narrow component fit) and Figure 3b (two narrow components fit), where the black, cyan, blue, green, orange, and red lines in the plot represent the observational data and fit to the power-law continuum, broad emission line, narrow emission lines, [O III] blue asymmetry component, and the combined model, respectively. The dotted line represents an absorption line component. It is found that the spectral decomposition with two narrow line components fit better ($\chi^2=2.0$) than

that with a single narrow line component ($\chi^2=6.7$). Our result emphasizes that the high-resolution spectral data is essential to identify closely-blended two narrow emission lines in dual black hole systems.

The blueshifted [O III] line could be coming from the offset AGN since the line strength of the blueshifted line is stronger than that of the redshifted one. The southern nucleus AGN is Compton thin (Juneau et al. 2011; $\log(L_{X\text{-ray}}/L_{[\text{OIII}]}) = 0.76$) based on the calculated Chandra ACIS-S point source sensitivity limit (4×10^{-15} ergs $\text{cm}^2 \text{s}^{-1}$ in 10^4 sec of exposure time and the redshifted [O III] flux from the spectral decomposition). The spectral line ratio of $\log([\text{O III}]/\text{H}\beta)$ is 0.99 and places the southern nucleus as a Seyfert 2 spectral type. The non-detection of $\text{H}\alpha$ broad-line and the X-ray in the Compton thin southern nucleus suggest it could be a low-luminosity AGN (LLAGN; $L_{\text{H}\alpha} < 10^{42}$ erg s^{-1}).

The stellar velocity dispersions σ_* of the southern and northern nuclei estimated from [O III] line width (Nelson & Whittle 1996, Greene & Ho 2005) are 165 km s^{-1} and 117 km s^{-1} , respectively. The black hole masses M_{BH} of the southern and northern nuclei estimated from the $M_{\text{BH}} - \sigma_*$ relation of elliptical galaxies (Kormendy & Ho 2013) are $\log(M_{\text{BH}}/M_{\odot})=8.11$ and $\log(M_{\text{BH}}/M_{\odot})=7.47$, respectively. The nuclear separation between two black holes is 1.26 kpc. If we assume they are moving in a circular orbit, then the orbital velocity from Kepler's law is only 23 km s^{-1} . If this is the case, then the observed velocity difference between two black holes will range from 0 to 46 km s^{-1} depending on the locations of the two SMBHs in the orbit and its inclination angle. The expected observed velocity difference will be $\sim 9 \text{ km s}^{-1}$ and can be calculated from the following expression:

$$bf46 \text{ km s}^{-1} \times \left(\frac{2}{\pi}\right)^2 \int_0^{\frac{\pi}{2}} \int_0^{\frac{\pi}{2}} \sin \theta \cos \phi \, d\phi d\theta,$$

where θ and ϕ are azimuthal angle and polar angle, respectively. However, the velocity difference measured from [O III] lines in the spectra is $233 \pm 30 \text{ km s}^{-1}$ ($\Delta\lambda = 3.9 \pm 0.5 \text{ \AA}$). If assuming two SMBHs orbiting each other, this velocity requires that the sum of two SMBH mass is larger than $10^9 M_{\odot}$. We argue that the offset AGN is not gravitationally bound with the black hole in the nucleus, but subject to gravitational potential of the host galaxy (i.e. not a binary black hole, but a dual black hole system).

If a galaxy surface brightness profile follows Sérsic model, we can express a ratio of the enclosed luminosity with radius r ($L(< r)$) and the total luminosity ($L(\text{total})$) as follows (e.g., Ciotti 1991; Ciotti & Bertin 1999; Graham & Driver 2005; Yoon et al. 2011):

$$L(< r) = L(\text{total}) \times \frac{\gamma(2n, x)}{\Gamma(2n)},$$

where γ , Γ , and n are incomplete gamma function, complete gamma function, and Sérsic index, respectively, and x is defined as follows, using shape parameter κ and effective radius

r_e :

$$x = \kappa \left(\frac{r}{r_e} \right)^{\frac{1}{n}}.$$

The shape parameter κ can be determined from the following formular (Ciotti & Bertin 1999; MacArthur et al. 2003):

$$\kappa \sim 2n - \frac{1}{3} + \frac{4}{405n} + \frac{46}{25515n^2} + \frac{131}{1148175n^3} - \frac{2194697}{30690717750n^4} + O(n^{-5}).$$

Then, if the stellar mass distribution follows the surface brightness distribution, the mass enclosed within the radius of r can be calculated by the following expression:

$$M(< r) = M(\text{total}) \times \frac{\gamma(2n, x)}{\Gamma(2n)}.$$

If the observed velocity difference is due to circular motion of the offset AGN with respect to the host galaxy’s stellar mass that is enclosed within a 1.26 kpc radius, then this enclosed mass should be $\sim 1.5 \times 10^{10} M_{\odot}$. By using κ , n and r_e (1.26 kpc) from Galfit (§3.2.1), the ratio between the mass enclosed within 1.26 kpc and the total mass is 7.4%, which implies that the total stellar mass of the host galaxy is $\sim 2.0 \times 10^{11} M_{\odot}$. The SDSS I band luminosity of the galaxy is $2.6 \times 10^{11} L_{\odot}$. If we adopt I band mass-to-light ratio of 1.7 (Shan et al. 2015), the estimated stellar mass based on I band luminosity is consistent with the inferred host galaxy mass.

3.2. Properties of the offset AGN (northern nucleus) and obscured AGN (host galaxy center)

3.2.1. Optical morphological properties

In the previous paper (Kim et al. 2017), we have performed a two-dimensional galaxy fitting with GALFIT 3.0 (Peng et al. 2010) and found the host galaxy is a bulge-dominated elliptical galaxy. In the fitting, we have used a single point spread function (PSF) component that corresponds to the offset AGN. Now, we have detected an optically hidden AGN in the center of the host galaxy and therefore have tried fitting the galaxy with two PSF components. However, introducing an additional PSF component does not produce a good fitting result, suggesting that the AGN in the host galaxy is deeply buried behind dust obscuration. The nondetection of the second broad line component in the KECK spectra supports this result. The host galaxy of the system can be well fitted with two galaxy components with two center positions: one centered at offset AGN and another centered at host galaxy center (top panel of Fig. 4). A Sersic index of $n=4$ fits well to the southern galaxy

that centers around the hidden AGN, and a Sersic index of $n=1$ fits well to the northern galaxy that centers around the offset AGN. Compared to the southern galaxy, which has a magnitude of $m_i=16.82$, the magnitude of the northern galaxy is $m_i=19.07$, indicating that the latter is significantly less luminous. If we assume both galaxy components have the same mass to light ratio, then their mass ratio is about 8 (black hole mass ratio is about 4.4). In addition, effective radius of the northern galaxy ($r_e=0''.35$) is significantly smaller compared to that of the southern nucleus ($r_e=2''.5$). The large differences in mass and effective radius between the two galaxies and a lack of long tidal tails that typically observed in major mergers (i.e. the Antennae galaxies) suggest this system is a result of minor merger.

In the fitting, we have set centers of southern and northern galaxies as a free parameter (two center positions) for the best fitting result. As a comparison, we have performed the Galfit with only one center position (i.e. the southern and northern galaxies have the same center position) and find that the result is comparable ($\chi^2 = 1.60$ vs. $\chi^2 = 1.63$ for the fit with two center positions and one center position, respectively), but slightly worse than that of the two center positions (bottom panel of Fig. 4). This result is expected due to the proximity of the two nuclei and the dominance of $n=4$ component in the fitting (i.e. coordinates of one center position falls near the center of the $n=4$ component).

3.2.2. Radio Properties of the Hidden AGN

The flux densities measured in the hidden AGN are 0.85 mJy, 0.63 mJy, and 0.24 mJy for 1.54 GHz, 10 GHz, and 33 GHz, respectively, assuming the VLBA is not resolving out any emission. The derived spectral indices α ($S_\nu \propto \nu^{-\alpha}$) are 0.16 and 0.81 for 1.54 GHz to 10 GHz and 10 GHz to 33 GHz, respectively. As suggested by the high brightness temperature $T_b = 7.2 \times 10^7$ K, the radio emission at 1.54 GHz would be dominated by non-thermal synchrotron emission. Thus, the flat spectral index at low frequencies can be explained by Synchrotron self-absorption in an optically thick environment as observed in many LLAGNs (i.e. Nagar et al. 2000). The steep spectral index of $\alpha = 0.81$ between 10 GHz and 33 GHz is typical for Synchrotron emission (Gioia et al. 1982; Klein et al. 2018). With decreasing frequency, the system is getting into a regime where the Synchrotron self-absorption is important and the spectral index becomes flat and turns over. The Synchrotron self-absorption that presumably occurs in the environment of large optical depth could explain a hidden AGN in the host galaxy, which is not seen in optical but seen in radio, in contrast to the off-nucleus AGN which is bright in optical but does not have a radio counterpart.

The radio source in the southern nuclei was resolved with the VLBA and its deconvolved size is $3.4 \text{ mas} \times 2.4 \text{ mas}$ corresponding to a physical scale of $17 \text{ pc} \times 12 \text{ pc}$. The 1.54 GHz

radio emission detected by the VLBA is originating from this small region. However, the flux density at 1.4 GHz (0.85 mJy) detected from the VLA Faint Images of the Radio Sky at Twenty centimetres (FIRST: Becker et al. 1995) survey is 1.61 ± 0.15 mJy. This is twice as large as the value detected with the VLBA at 1.54 GHz. The large synthesized beam size of FIRST ($5''.4$) that captures almost all of the radio emission in the galaxy could explain the difference of the flux densities. On the other hand, the intrinsic variability of the LLAGN could also explain the flux density difference (i.e. typical radio variability in LLAGN on a time scale of a few years is 20% to 70%: Falcke et al. 2001). The far-infrared (FIR) luminosity of this galaxy estimated from the IRAS measurements is $L_{FIR} = 10^{12.20} L_{\odot}$ and suggests the presence of significant star formation activity. Therefore, the additional radio emission of ~ 0.75 mJy measured by FIRST could be coming from the star formation-related activity (i.e. synchrotron radiation from Type II supernovae). The mean value of the q_{24} parameter ($\log(S_{24\mu m}/S_{1.4\text{GHz}})$; Ibar et al. 2008) of the star-forming galaxies is 0.95. The Spitzer/MIPS 24 μm flux density for CXO J101527.2+625911 is 6.3 mJy. If we assume that the excess 1.4 GHz emission measured by FIRST relative to the VLBA ($=0.75$ mJy) is all due to star formation, then $q_{24} = 0.92$; i.e., comparable to the q_{24} of star-forming galaxies. It could be possible that some fraction of the 24 μm flux density could come from offset AGN. In such a case, the q_{24} value could be smaller than measured.

4. Summary

We have carried out high resolution radio observations of CXO J101527.2+625911 previously claimed as a rSMBH candidate with the VLA and the VLBA and found the followings:

- A single compact radio source was detected from the VLA and the VLBA observations near the center of the host galaxy. The radio source is spatially resolved ($17 \text{ pc} \times 12 \text{ pc}$) with the VLBA and its brightness temperature is $T_b = 7.2 \times 10^7 \text{ K}$, which clearly indicates that the radio emission is from AGN. This combined with the Chandra-detected X-ray source associated with the northern offset AGN confirms that this system is a dual SMBH galaxy, not a rSMBH.

- Two narrow emission lines of $[\text{O III}]\lambda 5007\text{\AA}$ that were not seen in the SDSS spectrum were detected in the high resolution KECK spectra, supporting that this system is a dual SMBH galaxy. The velocity offset between the two narrow lines of $[\text{O III}]\lambda 5007\text{\AA}$ is $233 \pm 30 \text{ km s}^{-1}$.

- Morphological analysis of the HST image suggests this system has resulted from a minor merger, with a mass ratio of ~ 8 . The nuclear separation between the two nuclei is

$0''.26 \pm 0''.01$ (1.26 ± 0.05 kpc).

5. Acknowledgements

The authors thank the anonymous referee for comments and suggestions that greatly improved this paper. We also thank T. Treu and J.-H. Woo for sharing their reduced Keck spectra, and K. Nyland for helping preliminary reduction of VLBA data. This research has made use of the NASA/IPAC Extragalactic Database (NED) which is operated by the Jet Propulsion Laboratory, California Institute of Technology, under contract with the National Aeronautics and Space Administration. D.C.K., A.S.E., and S.S acknowledge support from the National Radio Astronomy Observatory (NRAO) and M.K. was supported by the National Research Foundation of Korea (NRF) grant funded by the Korea government (MSIT) (No. 2017R1C1B2002879). The National Radio Astronomy Observatory is a facility of the National Science Foundation operated under cooperative agreement by Associated Universities, Inc.

REFERENCES

- Baker, J. G., Boggs, W. D., Centrella, J., et al. 2008, *ApJ* 682, L29
- Becker, R. H., White, R. L., & Helfand, D. J. 1995, *ApJ*, 450, 559
- Callegari, S., Mayer, L., & Kazantzidis, S. et al. 2009, *ApJL*, 696, 89
- Campanelli, M., Lousto, C. O., Zlochower, Y., & Merritt, D. 2007, *PhRvL*, 98, 1102
- Ciotti, L. 1991, *A&A*, 249, 99
- Ciotti, L., & Bertin, G. 1999, *A&A*, 352, 447
- Condon, J. J., Huang, Z.-P., Yin, Q. E., & Thuan, T. X. 1991, *ApJ*, 378, 65
- Condon, J. J., 1992, *ARA&A*, 30, 575
- Deller, A. T., Brisken, W. F., Phillips, C. J., et al. 2011, *PASP*, 123, 275
- Falcke, H., Lehár, J., Barvainis, R., Nagar, N. M., & Wilson, A. S. 2001, *ASPC*, 224, 265
- Fomalont, E. B. 1999, in *ASP Conf. Ser.* 180, *Synthesis Imaging in Radio Astronomy II*, ed. G. B. Taylor, C. L. Carilli, & R. A. Perley (San Francisco, CA: ASP), 301
- Gaia Collaboration; Brown, A. G. A., Vallenari, A., & Prusti, T., et al. 2018, *A&A*, 616, 1
- Gioia, I. M., Gregorini, L., & Klein, U. 1982, *A&A*, 116, 164

Graham, A. W., & Driver, S. P. 2005, *PASP*, 22, 118
 Greene, J. E. & Ho, L. C. 2005, *ApJ*, 627, 721
 Greisen, E. W. 2003, *ASSL*, 285, 109
 Ibar, E., Cirasuolo, M., & Ivison, R. 2008, *MNRAS*, 386, 953
 Kim, D.-C., Yoon, Ilsang, & Evans, A. S. 2018, *ApJ*, 861, 51
 Klein, U., Lisenfeld, U., & Verley, S. 2018, *A&A*, 611, A55
 Kormendy, J., & Ho, L. 2013, *ARAA*, 51, 511
 Lousto, C. O., & Zlochower, Y. 2011, *PhRvL*, 107, 1102
 Ma, C., Arias, E. F., Bianco, G., et al. 2009, *ITN*, 35, 1
 MacArthur, L. A.; Courteau, S. & Holtzman, J. 2003, *ApJ*, 582, 689
 Merritt, D., Milosavljevic, M., Favata, M., Hughes, S. A., & Holz, D. E. 2004, *ApJ*, 607, 9
 Murphy, E. J., Condon, J. J., Schinnerer, E., et al. 2011, *ApJ*, 737, 67
 Nagar, N. M., Falcke, H., Wilson, A. S. & Ho, L. C., 2000, *ApJ*, 542, 186
 Nelson C. H., & Whittle M., 1996, *ApJ*, 465, 96
 Peng, C. Y., Ho, L. C., Impey, C. D., & Rix, H.-W. 2010, *AJ*, 139, 2097
 Schnittman, J. D. 2007, *ApJ*, 667, L133
 Shan, Y., McDonald, M., & Courteau, S. 2015, *ApJ*, 800, 122
 Walker, C. R. 1999, in *ASP Conf. Ser.* 180, *Synthesis Imaging in Radio Astronomy II*, ed. G. B. Taylor, C. L. Carilli, & R. A. Perley (San Francisco, CA: ASP), 433

This preprint was prepared with the AAS L^AT_EX macros v5.2.

Table 1. Summary of VLBA and VLA Observations

Tel.	Date	Position (J2000)		Band	On-source	Beam	PA	Flux density		RMS noise
(1)	(2)	R.A.	Dec.	(5)	hour	"	deg.	peak	total	mJy/beam
		(3)	(4)		(6)	(7)	(8)	(9)	(10)	(11)
VLBA	10/15/2017	10h15m27.267s	62d59m11.350s	L (0.256)	2.0	0.0125×0.005	175.7	0.74±0.03	0.85±0.05	0.03
VLA	03/07/2018	10h15m27.268s	62d59m11.348s	Ka (8.0)	0.6	0.06×0.05	58.3	0.26±0.01	0.24±0.01	0.008
VLA	03/07/2018	10h15m27.270s	62d59m11.351s	X (4.0)	0.5	0.22×0.17	55.1	0.61±0.03	0.63±0.05	0.005

(1) Telescope used. (2) Observing date. (3) Right Ascension. (4) Declination. (5) Radio band (Bandwidth in GHz unit): L: 18 cm, 1.54 GHz, Ka: 1 cm, 33.0 GHz, and X: 3.6 cm, 10.0 GHz. (6) On-source exposure time. (7) Synthesized beam size. (8) Position angle. (9) Peak (mJy/beam) and total (mJy) flux density. (10) RMS noise achieved.

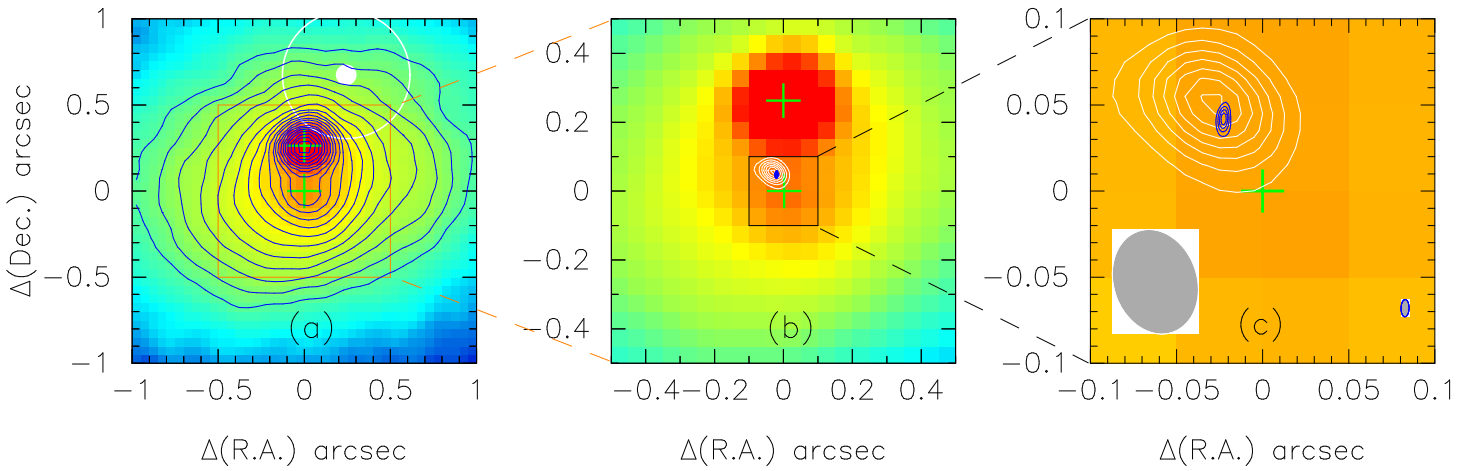


Fig. 1.— (a) The HST ACS I-band image of CXO J101527.2+625911, (b) Zoom-in image of the boxed region in panel (a), and (c) Zoom-in image of the boxed region in panel (b). The white dot and circle in panel (a) represent the location of the Chandra X-ray source and its positional uncertainty, which is $0''.32$. The green plus signs represent two nuclei: a northern nucleus (offset AGN) and a southern nucleus (nucleus in the center of the host galaxy). The white and blue contours in panel (b) represent VLA (33.0 GHz) and VLBA (1.54 GHz) continuum emission, respectively. The inset box in panel (b) is a zoomed-in view of the nuclear region. The synthesized beam sizes are plotted on the bottom-left (JVLA) and bottom-right (VLBA) in panel (c). Contour levels are spaced in log 0.15 units apart. North is up and east is to the left.

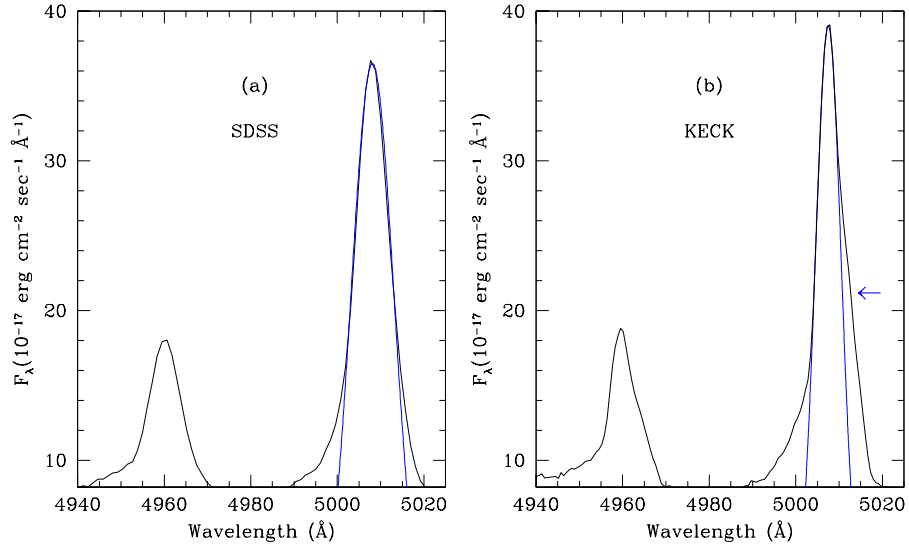


Fig. 2.— $[\text{O III}]\lambda 5007$ line in SDSS (a) and KECK (b) spectra fitted with a single Gaussian profile. An additional component is shown in the red part of the $[\text{O III}]\lambda 5007$ line in the KECK spectra, suggesting the existence of a second ionizing source.

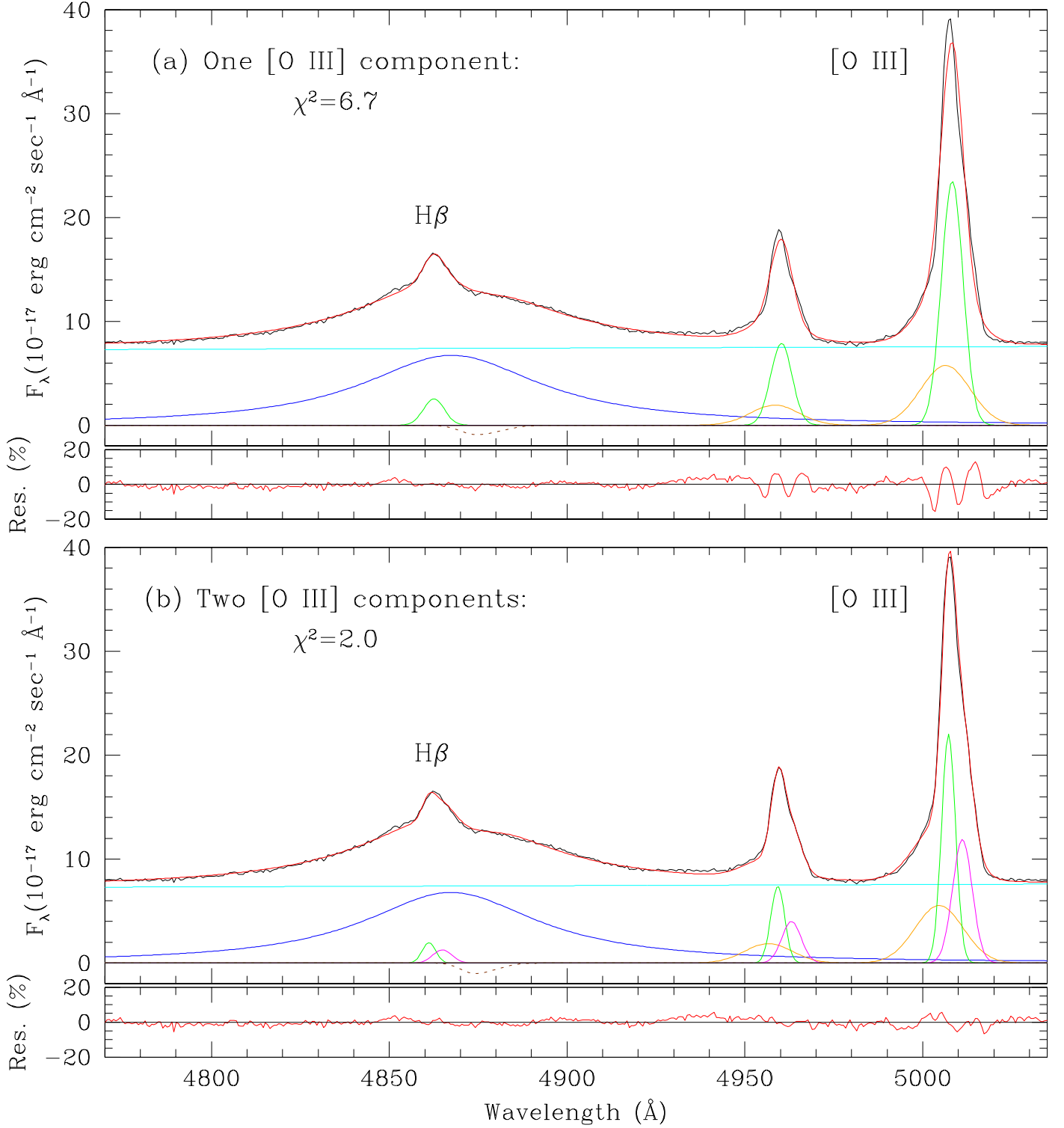
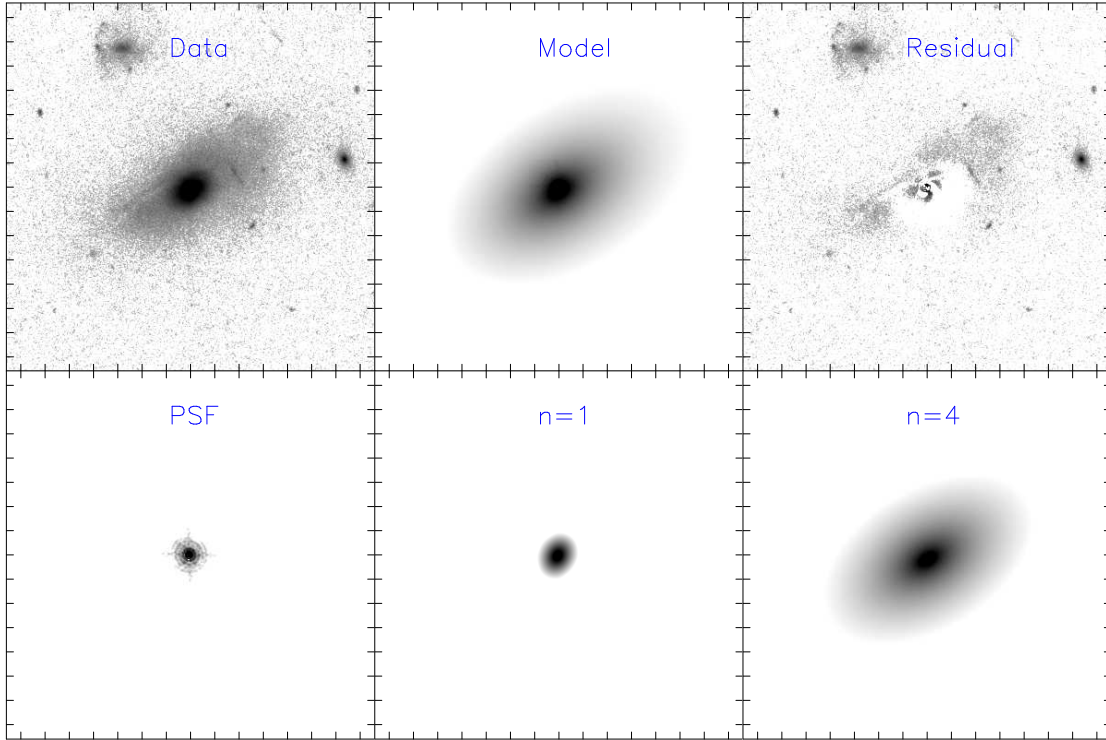


Fig. 3.— Result of spectral decompositions of the H β + [O III] region using a single [O III] component (a) and a double [O III] component (b). Black, cyan, blue, and red lines represent the data, power-law continuum model fit, broad emission line model fit, and the combined model fit, respectively. Green and magenta represent fit to the narrow emission lines and orange represents [O III] blue asymmetry component. The model fit with two [O III] components yields better result.

Galfit with two different centers ($\chi^2=1.60$)



Galfit with a single center ($\chi^2=1.63$)

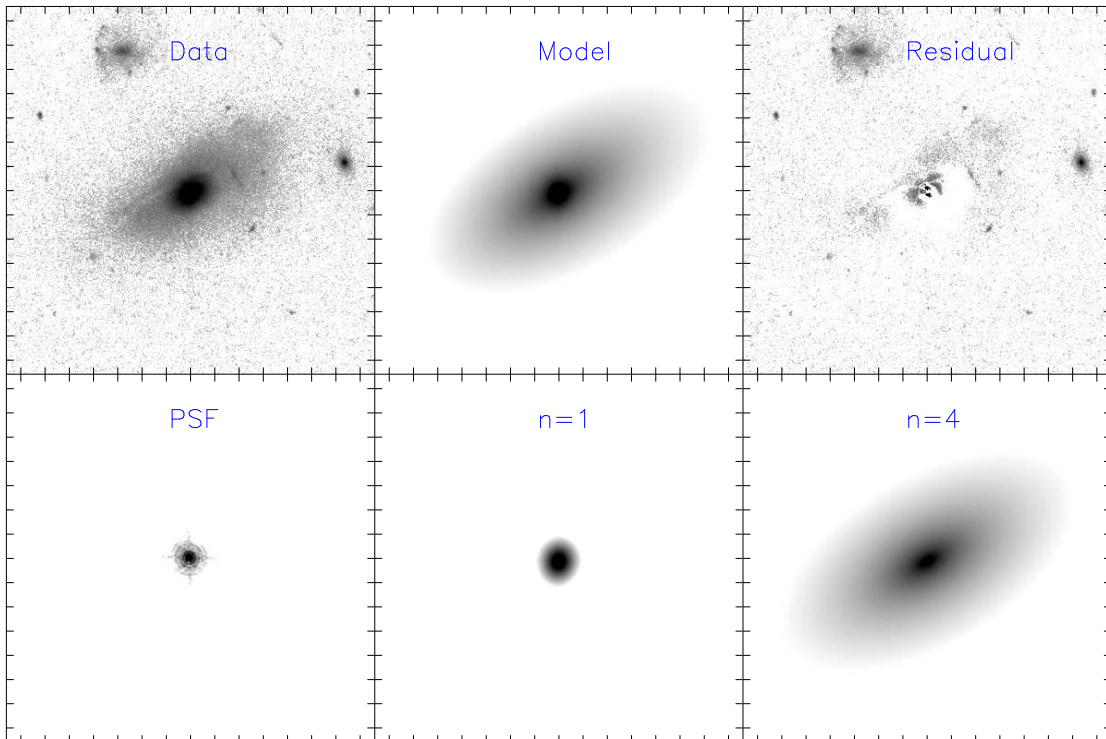


Fig. 4.— Results of Galfit with two centers (top panel) and with a single center (bottom